ICARUS 67, 264–280 (1986)

Bidirectional Reflectance Spectroscopy

4. The Extinction Coefficient and the Opposition Effect

BRUCE HAPKE

Department of Geology and Planetary Science, University of Pittsburgh, Pittsburgh, Pennsylvania 15260

Received January 27, 1986; revised April 28, 1986

The extinction coefficient and the opposition effect in a particulate medium are discussed. Simple analytic expressions that describe these quantities are rigorously derived using a few physically realistic mathematical approximations. The particles of the medium may have a distribution of sizes, and the particle density is allowed to vary with depth. The expression for the extinction coefficient is valid for both large and small porosities and is more accurate than the one commonly used. The opposition effect arises from the hiding of extinction shadows and occurs even if the particles are transparent. The angular half-width of the opposition peak is shown to be equal to the ratio of the average particle radius to extinction length at unit slant path optical depth in the medium, and depends on both the filling factor (ratio of bulk to solid density) F and the particle size distribution.

To illustrate the theory, it is fitted to observations of the Moon, an asteroid, and a satellite of Uranus; Europa is also discussed. For the Moon, a value of $F = 0.41$ is derived, in good agreement with data on Apollo soils. For Oberon, the width of the opposition effect peak gives $F = 0.10$, which is similar to values for terrestrial frosts and snow. Thus, the narrow opposition effects of the Uranian satellites do not require any unusual particles or microstructures on their surfaces. More photometric observations of Europa are needed.

I. INTRODUCTION

The opposition effect, or heiligenshein, is the surge in brightness of the light diffusely reflected from a surface near zero phase. It appears to be a nearly ubiquitous property of the bidirectional reflectance of natural materials. The phenomenon was first discovered by Seeliger (1876, 1895) in Saturn's rings. It has been observed on the Moon by many persons, including Gehrels *et al.* (1964), Whitaker (1969), and Wildey (1978); on asteroids by Gehrels *et al.* (1964), Bowell and Lumme (1979) and others; and on Mars by Thorpe (1978) and others. With the possible exception of Europa (Millis and Thompson, 1975; Buratti, 1985), it occurs in the photometeric function of every Solar System body whose regolith is visible. The brightness peak is especially narrow for at least three of the satellites of Uranus (Brown and Cruikshank, 1983). The opposition effect has also been observed on a wide variety of terrestrial materials (Hapke and Van Horn, 1963; Oetking, 1966; Egan and Hilgeman, 1976; Montgomery and Kohl, 1980).

The correct explanation was first given by Seeliger. In a particulate medium the interstices between the particles can be thought of as resembling "tunnels" through which light can penetrate. At large phase angles the interiors of most of the tunnels that the detector observes are in shadow, the light being blocked by the particles making up the walls of the tunnels. However, when the phase angle is less than, roughly, the ratio of the interparticle spacing to the extinction distance, the sides and bottoms of these tunnels are illuminated, resulting in enhanced brightness. Thus, the phenomenon may be thought of as caused by shadow hiding.

Seeliger's theory has been rediscussed by Irvine (1966). The opposition effect has also been discussed by many other persons, in-

0019-1035/86 $3.00

cluding Bobrov (1962), Hapke (1963), Whitaker (1979), Goguen (1981), Hapke (1981), and Lumme and Bowell (1981).

None of the theoretical treatments to date are completely satisfactory. Most assume that the particles are perfect spheres with no dispersion in particle size nor variation of particle density with depth allowed. Most ignore the effects of finite particle size and multiply scattered light on the amplitude of the brightness surge. In the treatment of Hapke (1963) the parameter that describes the angular width of the peak is difficult to relate to the physical properties of the scattering medium, and his rediscussion of this parameter in Hapke (1981) is incorrect. The treatments of Irvine (1966) and Lumme and Bowell (1981) are valid only when the porosity is large, as evidenced by the fact that their theories predict an appreciable effect even when the porosity is zero. A major difficulty, as emphasized by Whitaker (1979), is that the observed peaks are much narrower than these theories predict from measured porosities.

In this paper the opposition effect is reexamined theoretically for the case of the scattering of light from a semi-infinite, particulate medium with particles large compared to the wavelength. For visible light scattered from a regolith the treatment will also be valid if the particles are small compared to a wavelength, because such particles are cohesive and aggregate into clumps which behave like large grains. Because the opposition effect and the extinction coefficient are intimately related, the latter will be reexamined also. It will be shown that many of the above difficulties result because the expression commonly used for the extinction coefficient is incorrect. The filling in of the extinction shadows by multiply scattered light is taken into account. As with previous discussions in this series of papers (Hapke, 1981, 1984; Hapke and Wells, 1981), mathematical rigor is maintained wherever possible; however, the main goal of this paper is to obtain useful, approximate, analytic solutions that describe most real, physical situations with sufficient accuracy.

II. THE EXTINCTION COEFFICIENT OF A PARTICULATE MEDIUM

In virtually all treatments of scattering from a particulate medium the transmission T of a layer of thickness z for a ray of light incident on the slab from a direction making an angle θ with the normal to the layer is assumed to be given by

$$T = \exp\left(-\sec\theta \int_0^z E(z')dz'\right), \quad (1)$$

where the extinction coefficient E is assumed to be

$$E = n\langle\sigma\rangle, \quad (2)$$

where n is the number of particles per unit volume and $\langle\sigma\rangle$ is the average extinction cross section of the particles. It will be demonstrated that Eq. (2) is a limiting form that is valid only in the case of large porosity.

Consider a thin horizontal slab having thickness Δz bigger than the diameter of any particle and large lateral extent inside the medium (Fig. 1). The slab has a total volume U and contains a total of $N = nU$ particles, where $N \gg 1$. The particles may vary in size, shape, and composition, but are assumed to be equant and randomly oriented and positioned. The ith particle in the slab has volume V_i, where $V_i \ll U$, and extinction cross section σ_i. The extinction cross section is the product of the cross-sectional area of a particle and the extinc-

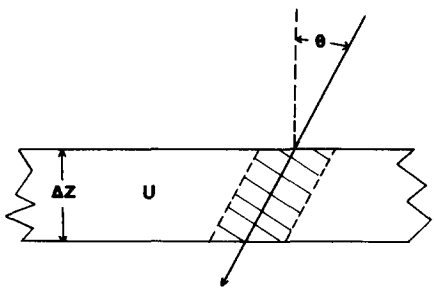

FIG. 1. Schematic diagram of the transmission through a slab of volume U containing particles.

tion efficiency. For particles large compared with a wavelength, the extinction efficiency is approximately equal to 2 if the particles are far apart, as in clouds or Saturn's rings, but must be taken to be unity if the particles are close together, as in a regolith (Hapke, 1981). For a nonspherical grain the extinction cross section is to be interpreted as the average area of the shadow the particle casts onto a screen at a distance of the order of the mean interparticle spacing $n^{-1/3}$ as the particle is oriented in all directions. The cross defined in this manner will be circular even for a nonspherical particle.

Consider a typical ray of light passing through the slab and making an angle θ with the normal to the slab. The transmission ΔT of the slab is the probability that the ray does not encounter a particle. This is equal to the probability that the center of any particle i in the slab is not in a circular cylinder axial to the ray with cross-sectional area σ_i and volume $\sigma_i \Delta z \sec \theta$.

In order to calculate this probability, imagine that the particles are all removed from the slab and then replaced randomly one at a time. Place the first particle in the slab. The probability that the center of this particle is not in the cylindrical volume $\sigma_1 \Delta z \sec \theta$ about the ray is

$$\Delta T_1 = \frac{U - \sigma_1 \Delta z \sec \theta}{U} = 1 - \frac{\sigma_1 \Delta z \sec \theta}{U}.$$

Next, place the second particle at a random position in the slab. Since the slab already contains one particle with volume V_1 and since the two particles cannot overlap, only a volume $U - V_1 - V_2$ is available to the center of the second. Thus, the probability that the second particle will not block the ray is equal to the probability that its center is not in the cylindrical volume $\sigma_2 \Delta z \sec \theta$ about the ray, or

$$\Delta T_2 = \frac{U - V_1 - V_2 - \sigma_2 \Delta z \sec \theta}{U - V_1 - V_2} = 1 - \frac{\sigma_2 \Delta z \sec \theta}{U - V_1 - V_2}.$$

Similarly, the probability that a third particle placed randomly in the slab will not block the ray is

$$\Delta T_3 = 1 - \frac{\sigma_3 \Delta z \sec \theta}{U - (V_1 + V_2 + V_3)}.$$

In general, the probability that the ith (where $i \neq 1$) particle will not block the ray is

$$\Delta T_i = 1 - \frac{\sigma_i \Delta z \sec \theta}{U - \sum_{j=1}^{i} V_j},$$

but since $U \gg V_1$, this relation is also valid for $i = 1$ with negligible error.

The probability that none of the N particles will block the ray is the product of the individual probabilities. Thus, the transmission of the slab for this particular sequence of drawing the particles is

$$\Delta T = \prod_{i=1}^{N} \left(1 - \frac{\sigma_i \Delta z \sec \theta}{U - \sum_{j=1}^{i} V_j} \right). \tag{3}$$

It is assumed that there is some void space within the slab, since otherwise it would be completely opaque and there would be no point in this calculation. Then U can always be taken large enough that $\left[U - \sum_{j=1}^{i} V_j \right] \gg \sigma_i \Delta z \sec \theta$ for any i. Note that this does not assume that the transmission ΔT of the slab cannot be small, only that the individual factors making up ΔT in (3) are close to unity. Then, to a good approximation,

$$\Delta T = \exp(-\Delta \tau \sec \theta), \tag{4a}$$

where

$$\Delta \tau = \frac{\Delta z}{U} \sum_{i=1}^{N} \frac{\sigma_i}{1 - \left(\sum_{j=1}^{i} V_j \right) / U}. \tag{4b}$$

Since the loading of the slab can be done in any order, to calculate $\Delta \tau$, all $N!$ permutations and combinations of the order in which the particles are placed must be cal-

culated and the average taken. It is convenient to carry out this averaging beginning with the last ($i = N$) term. This term is of the form $(\Delta z/U)\sigma_n \Big/ \left[1 - \left(\sum_{l=1}^{N} V_l\right)\Big/U\right]$. For each value of n this term occurs $(N-1)!$ times, because once n has been specified there are $(N-1)!$ ways to choose the earlier terms in (4b). Thus, the average of the $i = N$ term in (4b) carried out in this manner is

$$\Delta\tau_N = \frac{(N-1)!}{N!}\frac{\Delta z}{U}\sum_{n=1}^{N}\frac{\sigma_n}{1 - \left(\sum_{l=1}^{N} V_l\right)\Big/U}$$

$$= \frac{\Delta z}{U}\frac{\left(\sum_{n=1}^{N}\sigma_n\right)\Big/N}{1 - \left(\sum_{l=1}^{N} V_l\right)\Big/U} = \frac{\Delta z}{U}\frac{\langle\sigma\rangle}{1 - N\langle V\rangle/U},$$

where

$$\langle\sigma\rangle = \sum_{n=1}^{N}\sigma_n/N \tag{5}$$

is the average particle extinction cross section (weighted by number), and

$$\langle V\rangle = \sum_{l=1}^{N} V_l/N \tag{6}$$

is the average particle volume (weighted by number).

Continuing, the second to the last term ($i = N-1$) in (4b) is of the form $\left\{(\Delta z/U)\sigma_j \Big/ \left[1 - \left(\sum_{l=1}^{N} V_l - V_n\right)\Big/U\right]\right\}_{j\neq n}$. For each value of n and j this term occurs $(N-2)!$ times. Thus, the average value of the $i = N-1$ term in (4b) is

$$\Delta\tau_{N-1} = \frac{(N-2)!}{N!}\frac{\Delta z}{U}\sum_{j=1}^{N}\left[\sum_{\substack{n=1\\ n\neq j}}^{N}\frac{\sigma_j}{1 - \left(\sum_{l=1}^{N} V_l - V_n\right)\Big/U}\right].$$

Since $N \gg 1$, negligible error will result if in the last equation V_n is replaced by $\langle V\rangle$. Then this expression becomes

$$\Delta\tau_{N-1} \simeq \frac{(N-2)!}{N!}\frac{\Delta z}{U}\sum_{j=1}^{N}(N-1)\frac{\sigma_j}{1 - (N\langle V\rangle - \langle V\rangle)/U} = \frac{\Delta z}{U}\frac{\langle\sigma\rangle}{1 - (N-1)\langle V\rangle/U}.$$

Making similar approximations to calculate the average value of the $(N-k)$th terms gives

$$\Delta\tau_{N-k} \simeq \frac{\Delta z}{U}\frac{\langle\sigma\rangle}{1 - (N-k)\langle V\rangle/U}.$$

The relative error in the sums over the individual volumes in the denominators of each term in (4b) that results from replacing V_n by $\langle V\rangle$ becomes progressively larger as k increases. However, for large k these sums involve fewer particles and become progressively smaller compared with U. Also $\Delta\tau$ is dominated by the terms with small k. Hence, making this substitution in any of the terms will cause negligible error in $\Delta\tau$. Thus, to a sufficient approximation the last expression can be used to calculate the average of each term in (4b), giving

$$\Delta\tau = \frac{\Delta z}{U}\sum_{i=1}^{N}\frac{\langle\sigma\rangle}{1 - i\langle V\rangle/U}. \tag{7}$$

Expanding each fraction in (7) and rearranging gives

$$\Delta\tau = \frac{\Delta z\langle\sigma\rangle}{U}\left\{\left[1 + \left(\frac{\langle V\rangle}{U}\right) + \left(\frac{\langle V\rangle}{U}\right)^2 + \cdots\right] + \left[1 + \left(\frac{2\langle V\rangle}{U}\right) + \left(\frac{2\langle V\rangle}{U}\right)^2 + \cdots\right] + \cdots + \left[1 + \left(\frac{N\langle V\rangle}{U}\right) + \left(\frac{N\langle V\rangle}{U}\right)^2 + \cdots\right]\right\}$$

$$= \frac{\Delta z\langle\sigma\rangle}{U}\left\{N + \left(\frac{N\langle V\rangle}{U}\right)(1 + 2) + \cdots + N) + \left(\frac{N\langle V\rangle}{U}\right)^2(1^2 + 2^2 + \cdots + N^2) + \cdots\right\}.$$

Using the well-known relation [e.g., Dwight, 1947, Eq. (29.9)].

$$\sum_{n=1}^{N} n^j \simeq N^{j+1}/(j+1)$$

when $N \gg 1$, $\Delta\tau$ becomes

$$\Delta\tau \simeq \frac{\Delta z\langle\sigma\rangle}{U}\left\{N + \left(\frac{\langle V\rangle}{U}\right)\frac{N^2}{2} + \left(\frac{\langle V\rangle}{U}\right)^2\frac{N^3}{3} + \cdots\right\}$$

$$= \frac{\Delta z\langle\sigma\rangle}{\langle V\rangle}\left\{\left(\frac{N\langle V\rangle}{U}\right) + \frac{1}{2}\left(\frac{N\langle V\rangle}{U}\right)^2 + \frac{1}{3}\left(\frac{N\langle V\rangle}{U}\right)^3 + \cdots\right\}$$

$$= -\frac{\Delta z\langle\sigma\rangle}{\langle V\rangle}\ln\left(1 - \frac{N\langle V\rangle}{U}\right).$$

Define the filling factor F by

$$F = N\langle V\rangle/U = n\langle V\rangle. \tag{8}$$

Then $\Delta\tau = -n\langle\sigma\rangle\Delta z\ln(1-F)/F$, and

$$\Delta T = e^{(\Delta z \sec\theta n\langle\sigma\rangle/F)\ln(1-F)} = (1-F)^{(n\langle\sigma\rangle\Delta z\sec\theta)/F}. \tag{9}$$

Now, the probability of a ray penetrating a layer of finite thickness z of random particles is the product of the probabilities of penetrating a series of individual layers of thickness dz. Hence, the transmission of such a layer is

$$T = \exp\left[\sec\theta\int_0^z (n\langle\sigma\rangle/F)\ln(1-F)dz'\right]. \tag{10}$$

Comparing (10) with (1), it is seen that the more general expression for the extinction coefficient, which is valid for any particle spacing and size distribution, is

$$E = -n\langle\sigma\rangle\ln(1-F)/F, \tag{11}$$

where the filling factor F is the fraction of the volume occupied by particles. The porosity of the medium is $1-F$. When $F \ll 1$, $\ln(1-F) \simeq -F$, and E relaxes to its usual form [Eq. (2)]. However, as $F \to 1$ the layer becomes opaque.

Most discussions of radiative transfer in a particulate medium involve the assumption, either explicitly or implicity, that Eqs. (1) and (2) are correct. From (11) it is seen that such solutions of the radiative transfer equation remain valid, provided that in the extinction coefficient E the particle density n is replaced by an effective particle density n_e given by

$$n_e = -n\ln(1-F)/F. \tag{12}$$

III. THE OPPOSITION EFFECT

III.A. Derivation

In this section the singly scattered radiance from a semi-infinite, horizontally stratified medium will be calculated. Let the z direction be perpendicular to the strata, with z increasing upward. Let the medium be illuminated from above by a collimated source of light of intensity J and observed from above by a small detector with sensitive area da that accepts light from within a solid angle $d\omega$ (see Fig. 2). The incident radiation makes an angle i with z and the detector observes the surface at angle e. Let

$$\mu = \cos e \tag{13}$$

and

$$\mu_0 = \cos i. \tag{14}$$

Consider a slab of thickness dz located at position z within the medium. Then, from

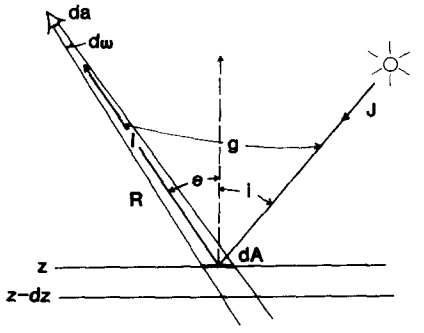

FIG. 2. Schematic diagram of scattering from a thin slab in a particulate medium.

the results of the previous section, the probability that an incident ray will penetrate to the slab is

$$T_i(z) = \exp(-\tau/\mu_0), \tag{15}$$

where τ is the optical depth to position z:

$$\tau(z) = \int_z^\infty n_e(z')\langle\sigma\rangle dz'. \tag{16}$$

Also, $d\tau = -n_e\langle\sigma\rangle dz$. Then the illuminance at the top of the slab at elevation z is JT_i. The illuminance at the lower face of the slab at $z - dz$ is $J \exp[-(\tau + d\tau)/\mu_0] = JT_i \exp(-d\tau/\mu_0)$, so that the amount of light per unit area perpendicular to J that interacts with particles in the slab is

$$JT_i[\exp(-d\tau/\mu_0) - 1] = JT_i d\tau/\mu_0.$$

The element of the slab in the field of view of the detector has volume $dA dz$, where $dA = R^2 d\omega/\mu$, and R is the slant distance from dA to the detector. The amount of light that interacts with particles in this volume is

$$-JT_i(d\tau/\mu_0)(dA\mu_0) = -JT_i d\tau dA.$$

Of this light, a fraction $wp(g)/4\pi$ is scattered per unit solid angle through phase angle g, where w is the average single scattering albedo and $p(g)$ is the average single particle angular scattering function; $p(g)$ is normalized so that its integral over all directions is 4π. Thus, the amount of light scattered by particles in the volume element toward the detector is

$$-JT_i d\tau R^2(d\omega/\mu)(da/R^2)wp(g)/4\pi = -J(w/4\pi)p(g)T_i(d\tau/\mu)da d\omega.$$

If each scattered ray exits the slab from a point widely separated from the point at which it entered then, according to the results of Section II, the probability that the ray scattered toward the detector will actually reach it is

$$T_e = \exp(-\tau/\mu). \tag{17}$$

This may occur, for instance, if a ray is refracted into the interior of a particle and emerges on the opposition side, or if a ray is scattered by a second particle before exiting the slab. In this case, the radiance (power per unit area per unit solid angle) at the detector from the slab is

$$dI = -J(w/4\pi)p(g)T_i T_e d\tau/\mu.$$

The total radiance is obtained by integrating the radiance from all slabs:

$$I(i, e, g) = J\frac{w}{4\pi}p(g)\int_0^\infty e^{-\tau/\mu_0}e^{-\tau/\mu}\frac{d\tau}{\mu} = J\frac{w}{4\pi}p(g)\frac{\mu_0}{\mu_0 + \mu}. \tag{18}$$

The factor $\mu_0/(\mu_0 + \mu)$ is the familiar Lommel–Seeliger law.

However, if the point at which a scattered ray leaves the slab is close to the point at which it entered, then T_e is not independent of T_i and is underestimated by (17). For instance, suppose a ray is scattered from the surface of a particle at point P and does not penetrate into its interior. Now, $T_i = \exp(-\tau/\mu_0)$ is the probability that no particle has its center in the cylinder whose axis is the ray connecting P with the source and having radius $\langle r\rangle$, where

$$\langle r\rangle = \sqrt{\langle\sigma\rangle/\pi} \tag{19}$$

is the effective particle radius, defined in terms of the average extinction cross section. If T_e were independent of T_i then, similarly, T_e would be the probability that no particle has its center in the cylinder with radius $\langle r\rangle$ and whose axis is the ray connecting P with the detector. However, portions of the two probability cylinders overlap. This is illustrated schematically in Fig. 3, in which the area $APBC$ is the cross section of the common volume U_c in the scattering plane (the plane containing the incident and scattered rays). This volume has been incorrectly counted twice in Eq. (18), so that the product of the incident and escape probabilities must be written

$$T_i T_e = \exp[-(\tau/\mu_0 - \tau/\mu - \tau_c)], \tag{20}$$

where τ_c is the integral of $n_e(z)$ over U_c.

The effect of the overlap can be calculated exactly when $g = 0$ and the direction

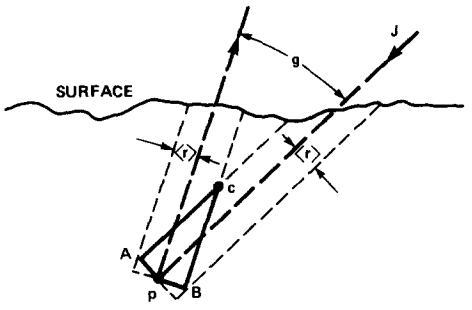

FIG. 3. Schematic diagram of a cross section through a point P in the scattering plane, showing the incident and escape probability cylinders and the common volume U_c.

to the detector is the same as the direction to the source. Then $\mu_0 = \mu$ and the two cylinders overlap completely, so that $\tau_c = \tau/\mu$, and

$$I(i, ,e, 0) = J\frac{w}{4\pi}p(0)\int_0^\infty e^{-\tau/\mu}\frac{d\tau}{\mu} = J\frac{w}{4\pi}p(0). \quad (21)$$

However, the incorrect equation (18) predicts that

$$I(i, e, 0) = J(w/4\pi)p(0)/2.$$

Thus, the opposition effect causes the singly scattered radiance to be twice as large at zero phase as would be calculated if the probability volume overlap were not taken into account.

One way of looking at the opposition effect is that the incident ray, in effect, preselects a preferential escape probability for rays escaping near zero phase. That is, if a ray is able to penetrate to depth z and illuminate a point there, than rays scattered from that same point back toward the direction of the source and within a small solid angle about that direction will be able to escape without being blocked by any particle. Another way of understanding the effect is that at zero phase all the extinction shadows are hidden by the objects that cast them.

It is sometimes erroneously stated that the opposition effect requires opaque particles. However, the shadows that are hidden are the extinction shadows. Thus, the effect occurs regardless of whether the particles are transparent or opaque. If the particles are transparent, multiply scattered light partially fills in these shadows, but cannot completely obliterate them. It may seem paradoxical that extinction causes a surface to brighten. The apparent paradox arises only if one attempts to treat a particulate medium as being continuous instead of remembering that it consists of discrete scatterers.

Irvine (1966) has given the mathematical expressions which describe the integral of particle density over the common volume for the case of a medium consisting of identical, perfectly spherical particles lying below a perfectly flat, horizontal boundary surface. The equations are complex and mathematically intractible, so that a computer is required for their solution. Irvine's equations have been evaluated numerically for a few special angles by Goguen (1981).

At this point it is appropriate to remember the actual geometry inside a real particulate medium. The particles are not spheres. The interstices between the particles through which the light penetrates into the interior of the medium have cross sections that are not perfectly round, nor cusp shaped, but extremely irregular. Moreover, the surface of any planetary regolith or laboratory powder is not a perfectly flat plane, but is very irregular, especially on a small scale. Thus, the rigorous mathematical formalism of Irvine (1966) and Goguen (1981) is not necessarily a better description of physical reality than an appropriate approximate solution that is mathematically tractable.

The cross section $APBC$ of U_c through the scattering plane containing point P is shown in Fig. 3. It consists of two right triangles with sides $\langle r\rangle$ and $\langle r\rangle \cot(g/2)$, with common hypotenuse $s = PC = \langle r\rangle \csc(g/2)$ and area $\langle r\rangle^2 \cot(g/2)$. Let z_1 be the projection of s onto the vertical axis. Then z_1 is given by the following system of simulta-

neous equations:

$$q^2 = \frac{z_1^2}{\mu^2} + \langle r\rangle^2 \csc^2\frac{g}{2} - 2\frac{z_1 \cos\frac{g}{2}}{\mu}\langle r\rangle \csc\frac{g}{2}$$
$$= \left(\frac{z_1}{\mu} - \langle r\rangle \cot\frac{g}{2}\right)^2 + \langle r\rangle^2$$

$$q_0^2 = \frac{z_1^2}{\mu_0^2} + \langle r\rangle^2 \csc^2\frac{g}{2} - 2\frac{z_1 \cos\frac{g}{2}}{\mu_0}\langle r\rangle \csc\frac{g}{2}$$
$$= \left(\frac{z_1}{\mu_0} - \langle r\rangle \cot\frac{g}{2}\right)^2 + \langle r\rangle^2$$

$$(q + q_0)^2 = z_1^2(\tan^2 i + \tan^2 e - 2\tan i \tan e \cos\phi)\cos g = \cos i \cos e + \sin i \sin e \cos\phi,$$

where q is the distance from C to the intersection of the exit ray with the horizontal plane containing C, q_0 is the corresponding distance for the incident ray, and ϕ is the azimuth angle between the projections of the incident and exit rays on the horizontal plane.

Near $g = 0$, $\cot(g/2) \gg 1$, so that

$$q \simeq \pm[z_1/\mu - \langle r\rangle \cot(g/2)]$$

and

$$q_0 \simeq \mp[z_1/\mu_0 - \langle r\rangle \cot(g/2)],$$

where the positive sign is to be used for q and the negative sign for q_0 if $e > i$, and oppositely if $i > e$. When g is small each term on the right hand side of the last two equations is large, but both q and q_0 are small. Hence, the difference between q and q_0 will be small also, and to a sufficient approximation

$$|q - q_0| \simeq z_1/\mu_0 + z_1/\mu - 2\langle r\rangle \cot(g/2) \simeq 0,$$

so that

$$z_1 \simeq \langle\mu\rangle\langle r\rangle \cot(g/2), \tag{22}$$

where

$$1/\langle\mu\rangle = (1/\mu_0 + 1/\mu)/2 \quad \text{or} \quad \langle\mu\rangle = 2\mu_0\mu/(\mu_0 + \mu). \tag{23}$$

This approximate expression for z_1 is good when g is small. It is poor when g is large and the incident and exit rays are on opposite sides of the normal. However, when g is large the opposition sides effect makes only a small contribution to the brightness. Hence, (22) will cause negligible error in the total radiance for any g.

At any altitude z' between z and $z + z_1$, a horizontal cut through the common volume U_c consists of two overlapping ellipses. The thickness of the overlapping area in the direction perpendicular to the scattering plane changes much less rapidly with z' than the width in directions parallel to the scattering plane. Hence, U_c will be approximated by a volume which is a triangle in planes parallel to the scattering plane and with constant thickness b, where b will be determined below, perpendicular to the scattering plane. This approximation essentially involves replacing the ellipses by rectangles. The triangular cross section will be required to have the same area, $\langle r\rangle^2 \cot(g/2)$, and altitude, z_1, as $APBC$, and its base to be in the z plane. Then

$$U_c \simeq b\langle r\rangle^2 \cot(g/2). \tag{24}$$

The part of the common volume lying above any plane at z' between z and $z + z_1$ is

$$U_a(z') = U_c[1 - (z' - z)/z_1]^2,$$

so that

$$dU_a(z') = -2U_c[1 - (z' - z)/z_1]dz'/z_1 = -(2b\langle r\rangle/\langle\mu\rangle)[1 - (z' - z)/z_1]dz'.$$

Thus, the quantity which must be subtracted from the total optical depth is

$$\tau_c = -\int_z^{z+z_1} n_e \frac{2b\langle r\rangle}{\langle\mu\rangle}\left(1 - \frac{z' - z}{z_1}\right)dz'. \tag{25}$$

The thickness b of the common volume is determined by requiring that at $g = 0$, when $\mu_0 = \mu = \langle\mu\rangle$ and $z_1 \to \infty$, then $\tau_c = \tau/\mu$, or

$$\int_z^\infty n_e \frac{2b\langle r\rangle}{\langle\mu\rangle}dz' = \frac{1}{\mu}\int_z^\infty ne\langle\sigma\rangle dz'.$$

Thus,

$$b = \langle\sigma\rangle/2\langle r\rangle = \pi\langle r\rangle/2, \tag{26}$$

so that

$$\tau_c = -\frac{1}{\langle\mu\rangle}\int_z^{z+z_1} n_e\langle\sigma\rangle\left(1 - \frac{z' - z}{z_1}\right)dz'$$
$$= \frac{1}{\langle\mu\rangle}\int_{\tau(z)}^{\tau(z+z_1)}\left(1 - \frac{z' - z}{z_1}\right)d\tau(z'). \tag{27}$$

Integrating (27) by parts gives

$$\tau_c = -\tau/\langle\mu\rangle + \tau'/\langle\mu\rangle, \tag{28}$$

where

$$\tau' = \frac{1}{z_1}\int_z^{z+z_1}\tau(z')dz'. \tag{29}$$

Inserting this result into Eq. (20) gives

$$\tau/\mu_0 + \tau/\mu - \tau_c = (\tau + \tau')/\langle\mu\rangle.$$

Thus, the singly scattered radiance can be written

$$I(i, e, g) = J\frac{w}{4\pi}p(g)\int_0^\infty e^{-(\tau+\tau')/\langle\mu\rangle}\frac{d\tau}{\mu}. \tag{30}$$

In the remainder of this section Eqs. (29) and (30) will be evaluated for several different distributions of effective particle density $n_e(z)$ with depth.

III.B. Step-Function Distribution

Suppose the effective density can be approximated by a step function:

$$z \geq 0\text{: } n_e(z) = 0,$$
$$z < 0\text{: } n_e(z) = n_e = \text{constant}.$$

This is the case usually considered in theoretical discussions of the opposition effect. Then

$$z \geq 0\text{: } \tau' = 0,$$
$$-z_1 < z < 0\text{: } \tau' = \tau^2/2\tau_1,$$
$$z \leq -z_1\text{: } \tau' = \tau - \tau_1/2,$$

where

$$\tau_1 = n_e\langle\sigma\rangle z_1 \tag{31}$$

and z_1 is defined by (22).

Then (28) may be readily evaluated to give

$$I(i, e, g) = J\frac{w}{4\pi}p(g)\frac{\mu_0}{\mu_0 + \mu}[1 + B(g)], \tag{32}$$

where

$$1 + B(g) = \sqrt{\frac{2\pi}{\upsilon_s}}\,e^{1/2\upsilon_s}\left[\text{erf}\sqrt{\frac{2}{\upsilon_s}} - \text{erf}\sqrt{\frac{1}{2\upsilon_s}}\right] + e^{-3/2\upsilon_s}, \tag{33}$$

and,

$$\upsilon_s = \langle\mu\rangle/\tau_1 = \tan\left(\frac{g}{2}\right)\Big/ n_e\langle\sigma\rangle\langle r\rangle. \tag{34}$$

Equation (33) for $[1 + B(g)]$ for a step-function distribution is plotted versus $\upsilon = \upsilon_s$ in Fig. 4. It is sharply peaked with value 2 at $\upsilon = 0$ and decreases rapidly to value 1 as υ and g increase.

Equation (34), although analytic, is inconvenient because most personal computers and programmable calculators do not have a subroutine for the error function. It is found that, to better than 3%

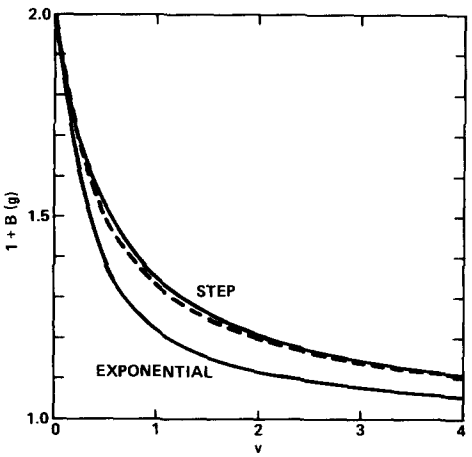

FIG. 4. Plot of the opposition effect function $[1 + B(g)]$ versus the generalized angular parameter υ for the step function ($\upsilon = \upsilon_s$) and exponential ($\upsilon = \upsilon_e$) particle density–depth distributions (solid lines). The dashed line is a plot of the empirical function $[1 + 1/(1 + 2\upsilon)]$. See the text for definitions of υ_s and υ_e.

everywhere, (33) may be approximated by

$$[1 + B(g)] = 1 + 1/(1 + 2v_s). \quad (35)$$

This expression, which is shown as the dashed line in Fig. 4, is much more convenient and probably is not distinguishable from Eq. (33) in practice.

III.C. Exponential Distribution

Suppose the density can be characterized by an exponential distribution:

$$n_e(z) = n_0 \exp(-z/\lambda), \quad (36)$$

where λ is a scale height. This case probably would not be applicable to a regolith, but might describe a dense, low-lying haze or suspended dust. Then (29) is

$$\tau' = -\frac{\lambda}{z_1}(e^{-(z+z_1)/\lambda} - e^{-z/\lambda}) = \frac{\lambda}{z_1}\tau(z)(1 - \tau_e), \quad (37)$$

where

$$\tau_e = \exp(-z_1/\lambda), \quad (38)$$

and z_1 is defined by (22). Equation (37) may be inserted into (30) to give an expression of the same form as (32) but with the following instead of (33),

$$1 + B(g) = 2[1 + v_e(1 - e^{-1/v_e})]^{-1}, \quad (39)$$

where

$$v_e = \langle\mu\rangle\langle r\rangle \tan(g/2)/\lambda. \quad (40)$$

Equation (39) for $[1 + B(g)]$ is plotted in Fig. 4 versus $v = v_e$.

III.D. Hyperbolic Tangent Distribution

Neither the step function nor the exponential distributions are particularly physically realistic, their main virtue being that the resulting opposition effects can be calculated analytically. While the surface of any powder is irregular on the scale of a few particle diameters, this is especially true for fine-grained, cohesive soils. Unless extreme care is taken to deposit and smooth a fine powder in either the laboratory or in nature, its surface is poorly described by a step function. Rather, the mean density decreases gradually with a very intricate microstructure over a distance of many particle diameters. This gives rise to the well-known "fairy castle structures" described by Hapke and Van Horn (1963). Thus, in general, the particle density would be described more accurately by a function which decreases gradually to zero from a saturated value in the interior of the powder. These considerations suggest that a more realistic distribution is

$$n_e = (n_0/2)[1 - \tanh(z/2L)], \quad (41)$$

where L is a length that characterizes the density distribution. When $z/L \ll -1$, $n_e = n_0$, and when $z/L \gg 1$, $n_e = n_0 \exp(-z/L)$.

Inserting (41) into (29) and (30) gives an equation of the same form as (32), but where $[1 + B(g)]$ can be put into the following form:

$$1 + B(g) = y\int_{-\infty}^{\infty} \exp\left\{-y\left[\ln(1 - e^{-x}) + u\int_x^{x+1/u} \ln(1 + e^{-x'})dx'\right]\right\}\frac{dx}{1 + e^x}, \quad (42)$$

where

$$x = z/L, \qquad y = n_0\langle\sigma\rangle L/\langle\mu\rangle, \qquad u = L/z_i. \quad (43)$$

This integral was evaluated numerically for values of u between 0 and 4 and y between 0.1 and 10. It was found that $[1 + B(g)]$ can be represented quite closely by the empirical expression

$$[1 + B(g)] = 1 + 1/(1 + 2v_t), \quad (44)$$

where

$$v_t = \left(1 + \frac{5}{3}y\right)\frac{u}{y} = \left(1 + \frac{5}{3}\frac{n_0\langle\sigma\rangle L}{\langle\mu\rangle}\right)\frac{\tan\frac{g}{2}}{n_0\langle\sigma\rangle\langle r\rangle}. \quad (45)$$

Calculated values of $[1 + B(g)]$ are plotted as a function of $v = v_t$ in Fig. 5, along with the empirical curve [Eq. (44)].

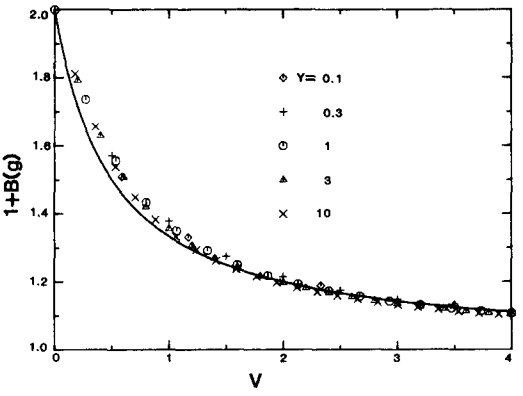

FIG. 5. Plot of the opposition effect function [1 + $B(g)$] versus the generalized angular parameter $v = v_t$ for a hyperbolic tangent particle density–depth distribution. The symbols correspond to different values of the parameter $y = n_0\langle\sigma\rangle L/\langle\mu\rangle$. The solid line is a plot of the empirical function [1 + 1/(1 + 2v)]. See the text for the definition of v_t.

IV. THE ANGULAR WIDTH OF THE OPPOSITION EFFECT

In the remainder of this paper the exponential distribution will not be considered further because there are probably few real circumstances to which it would apply. For the cases of both the step function and hyperbolic tangent distributions the opposition effect can be represented by an expression of the form

$$B(g) = 1/[1 + \tan(g/2)/h)] \qquad (46)$$

where for the step-function distribution

$$h = n_e\langle\sigma\rangle\langle r\rangle/2 \qquad (47)$$

and for the more general tanh distribution

$$h = n_0\langle\sigma\rangle\langle r\rangle/2(1 + 5n_0\langle\sigma\rangle L/3\langle\mu\rangle), \qquad (48)$$

where n_e is given by (12). The half-width of the peak is given approximately by

$$\Delta g = 2h. \qquad (49)$$

For the step-function distribution the width of the opposition effect is determined by the ratio of the mean particle radius $\langle r\rangle = \sqrt{\langle\sigma\rangle/\pi}$ to the extinction length $1/n_e\langle\sigma\rangle$. The width parameter h for the tanh distribution relaxes to the step-function expression when the distance over which the particle density decreases from its saturation value, characterized by L, is small compared with the saturation extinction length $1/n_0\langle\sigma\rangle$. However, when this latter ratio is large, as could be the case in a cohesive, fairy-castle-surfaced regolith, then $h \simeq 0.3\langle\mu\rangle\langle r\rangle/L$, and the width for the tanh distribution is much smaller than for the step-function distribution. For this case, the width also depends on position through the parameter $\langle\mu\rangle$, because near the limb or terminator the effective density illuminated or seen along a slant path is at higher altitude and, thus, is smaller than at the center of the disk.

The meaning of the angular width parameter h for the tanh distribution may be clarified by calculating the value of $n_e(\tau/\langle\mu\rangle)$ at the level where the slant path optical depth $\tau/\langle\mu\rangle = 1$. A straightforward calculation gives

$$n_e(1) = n_0[1 - \exp(-\langle\mu\rangle/n_0\langle\sigma\rangle L)].$$

When $n_0\langle\sigma\rangle L/\langle\mu\rangle \ll 1$, then $n_e(1) = n_0$; a step-function distribution with the same density would have $h = n_e(1)\langle\sigma\rangle\langle r\rangle/2 = n_0\langle\sigma\rangle\langle r\rangle/2$. As $n_0\langle\sigma\rangle L/\langle\mu\rangle$ increases, $n_e(1)$ decreases. When $n_0\langle\sigma\rangle L/\langle\mu\rangle \gg 1$, then $n_e(1) = \langle\mu\rangle/\langle\sigma\rangle L$, so that the equivalent step-function expression is $h = n_e(1)\langle\sigma\rangle\langle r\rangle/2 = 0.5\langle\mu\rangle\langle r\rangle L$, which, to within a factor of $\frac{3}{5}$ is identical to the value given in the preceding paragraph. Thus, in giving a physical interpretation to h, the expression for the step-function distribution [Eq. (47)] may be used, provided n_e is interpreted to be the value at the level where the slant path optical depth is unity, and not as the compacted value at depth. Henceforth, with this proviso, the conceptually simpler step-function equation for h will be used.

From Eqs. (47) and (12), it can be seen that as the filling factor F increases, the angular width increases also. The opposition effect disappears for a solid surface when $F = 1$. As the particle density decreases, the peak narrows. However, the width cannot become indefinitely small because the peak must be averaged over the finite angular

widths of the source and detector. This averaging reduces the measured amplitude and requires that the width not be less than the sum of the half-widths of the source and detector as seen from the surface.

If the particle size distribution is narrow and the particles are equant, then $n\langle\sigma\rangle\langle r\rangle/F = \langle\sigma\rangle\langle r\rangle/\langle V\rangle = \frac{3}{4}$ and $h = -3\ln(1 - F)/8$. For a close-packed powder ($F \simeq \frac{1}{2}$), the half-angle is about 30°, which is much broader than most observed peaks.

A broad distribution of particle sizes will reduce the peak half-width. This can be seen because $\langle\sigma\rangle$ and $\langle r\rangle$ tend to be dominated by the smaller sizes, while $\langle V\rangle$ tends to emphasize the larger sizes. For a power-law particle size distribution

$$n(r)dr = Kr^{-\beta}dr, \tag{50}$$

the width depends on both the exponent β and on the ratio r_l/r_s of the largest to smallest, respectively, particle sizes in the distribution. If $\beta \leq 1$ or $\beta > 4$, then the largest or smallest sizes, respectively, dominate the distribution and h is not much smaller than if the size distribution is narrow. However, if $1 < \beta \leq 4$ and r_l/r_s is large, then Δg can be quite narrow. Expressions for h for several different particle size distribution functions are given in Table I.

A particularly interesting situation occurs when $\beta = 4$. This case is important because it is the distribution which tends to result from comminution. It characterizes lunar soil (Bhattacharya *et al.*, 1975) and probably the surfaces of many other bodies in the Solar System as well. In this case $\langle\sigma\rangle\langle r\rangle$ and $\langle V\rangle$ are considerably different. From Table I,

$$h = -3\sqrt{3}\ \ln(1 - F)/8\ln(r_l/r_s). \tag{51}$$

If $r_l/r_s = 1000$ and $F = \frac{1}{2}$, then $h = 0.065$ and the width of the peak is only about 7°, instead of 30°.

Whitaker (1979) has emphasized the problem of accounting for the narrow brightness surges observed on bodies of the Solar System using previously published theories and has even questioned whether shadow hiding is the correct explanation. However, the present discussion shows that there is no difficulty in obtaining very narrow opposition effects from soils when the effects of particle size distributions are taken into account and the bulk density is allowed to vary with depth.

TABLE I

ANGULAR WIDTH PARAMETER h FOR VARIOUS PARTICLE SIZE DISTRIBUTIONS

Distribution $n(r)$	$h = -(\frac{3}{8})\ln(1 - F)Y$ Y	$Y(r_l/r_s = 1000)$
$K\delta(r - \bar{r})$	1	1
$Kr\exp(-r/\bar{r})$	$\sqrt{\frac{3}{8}}$	0.612
$Kr^{-\beta}$: β		
0	$4/3\sqrt{3}$	0.770
1	$3/\sqrt{8\ln(r_l/r_s)}$	0.404
2	$2\sqrt{r_s/r_l}$	0.0632
3	$\sqrt{2}[\ln(r_l/r_s)]^{3/2}(r_s/r_l)$	0.0257
4	$\sqrt{3}/\ln(r_l/r_s)$	0.251
5	$1/\sqrt{2}$	0.707

V. THE AMPLITUDE OF THE OPPOSITION EFFECT

According to the approximate equations developed in this paper, the opposition effect is as strong at the limb as anywhere else on a planet. The numerical evaluations by Goguen (1981) of the exact expressions of Irvine (1966) show that this result is correct. This is in contrast to the model of the opposition effect derived by Lumme and Bowell (1981) that predicts no brightness surge near the limb.

As shown rigorously in Section III, the maximum increase in brightness that can be attributed to shadow hiding between soil particles is a factor of 2, corresponding to a magnitude change of $\Delta m = 0.753$; a greater surge than this must have other causes. Potential additional factors include the following: shadow hiding in complex, porous particles (Whitaker, 1979), so that the single particle scattering function itself has an opposition effect; glory-like backscatter from spherical particles (Oetking, 1966); and in-

ternal retroreflections from particles with shapes that act like corner reflections (Trowbridge, 1978).

There are a number of factors that will decrease the amplitude of the opposition effect. First, the opposition effect acts only on the singly scattered radiance. For multiply scattered light the probability cylinders have paths within the medium from one particle to another so that the probability that the initial incident and final escape cylindrical volumes overlap is negligible. Esposito (1979) has carried out numerical calculations in which probability cylinder overlap was included in twice-scattered light, and found negligible effect on the reflectance. Physically, the multiply scattered light partly fills in the shadows, so that the opposition effect is reduced in amplitude, but not completely eliminated. Mathematically, this means that the opposition effect factor multiplies only the singly scattered component of the bidirectional reflectance function, but not the multiply scattered portion.

Second, if the particles are too far apart, then the shadows that one particle casts on another are filled in. As discussed in detail in Hapke (1981), this can be done both by forward scattered light diffracted around the edges of the particles or by the penumbra caused by the finite angular sizes of the source and/or the detector. For this reason clouds and hazes usually do not have an opposition effect, but regoliths do. This provides a way of telling whether one is observing a cloud cover or regolith on an unresolved body in the Solar System.

Third, if the particles are far enough apart that they essentially act like points to the incident and escaping ray bundles, then all of the light back scattered by the particle takes part in the opposition effect. However, if the particles are so close together that only parts of them are illuminated or observed, then the refracted light that penetrates into the interior of an individual grain will, in general, emerge from that grain at a considerable distance from the entry point. In this case the incident and escape probability cylinders will have negligible overlap. Hence, only the light reflected or scattered from very close to the surfaces of the particles contributes to the opposition effect.

There are several observations which support the reality of the last factor. Hapke and Wells (1981) measured the amplitude of the opposition effect, as well as w and $p(g)$, for cobalt-doped silicate glass powders at several wavelengths. It may readily be seen from inspection of their data that the amplitude increases both as w decreases and also as the particles become more forward scattering. For smooth-surfaced particles large compared with a wavelength the surface component of the light scattered from them is proportional to the Fresnel reflectivity, which increases with phase angle. Thus, as w decreases, the component of the light scattered from the interior decreases and a greater fraction of the scattered light comes from the surface. If the particles have smooth surfaces the surface-reflected Fesnel component is forward scattering. On the other hand, if the particles have rough surfaces that cause shadowing, the surface component will be back scattering. The particles studied by Hapke and Wells (1981) had relatively smooth surfaces.

Montgomery and Kohl (1980) illuminated a variety of surfaces with linearly polarized light and measured the scattered radiance in the same and perpendicular polarization directions. They found that only the light scattered with the same direction of polarization had an opposition effect. Fresnel surface reflections tend to preserve the polarization, but light refracted any distance into a particle and scattered, reflected, or refracted there tends to have its polarization vector randomly rotated.

In order to describe mathematically the effect of the finite sizes of the particles, it is assumed that, to a first approximation, the amplitude and angular dependences can be separated. This assumption is reasonable

because for large irregular particles, $p(g)$ is not a rapidly varying function of g around zero phase. Then, instead of (46), the opposition effect must be written

$$B(g) = B_0/[1 + \tan(g/2)/h], \quad (52)$$

where B_0 is the ratio of the near-surface contribution to the total particle scattering at zero phase:

$$B_0 = S(0)/wp(0), \quad (53)$$

and $S(0)$ is the fraction of the light scattered from close to the surface of the particle at $g = 0$.

If the particles are opaque then all of the scattered light comes from the surface; in that case $S(0) = wp(0)$ and $B_0 = 1$. A lower limit to $S(0)$ will be the Fresnel reflection from the particle surface facets

$$F_r = [(n - 1)^2 + k^2]/[(n + 1)^2 + k^2], \quad (54)$$

where n and k are, respectively, the real and imaginary parts of the refractive index. In addition to F_r, however, the optical interface may also involve scattering from microscopic defects located at or just under the particle surface, such as asperities or cracks induced by grinding. Such defects would, in the first approximation, tend to preserve the direction of polarization, while increasing $S(0)$ over F_r. This would explain the curious observation of Oetking (1966) that granulated sugar having particles with smooth surfaces had a much smaller opposition effect than sugar with crystals whose surfaces were described as being frosted and pitted.

In a previous paper (Hapke, 1981), I introduced the concept of the amplitude term B_0. However, in that paper the angular dependence of $B(g)$ was based on a previous (Hapke, 1963), less rigorous derivation. Also, B_0 was empirically estimated to be given by $B_0 \simeq \exp(-w^2/2)$, based on the observed correlation with w in the cobalt glass. That discussion is now seen to be only partly correct and that empirical expression should not be used.

VI. APPLICATIONS

In Hapke (1981) a theory of diffuse scattering from particulate media was derived. The scattered radiance is given by

$$I = J \frac{w}{4\pi} \frac{\mu_0}{\mu_0 + \mu} \{[1 + B(g)]p(g) + H(\mu_0)H(\mu) - 1\}, \quad (55)$$

where $H(x) = [1 + 2x]/[1 + 2x\sqrt{1 - w}]$. The part of this equation proportional to $p(g)$ is due to the singly scattered radiation, while that proportional to $[H(\mu_0)H(\mu) - 1]$ is due to the multiply scattered radiation. In accordance with the preceding discussion, the opposition effect should be included by multiplying only the single scattering part by $[1 + B(g)]$, as has been done in (55). The equations in Hapke (1981) were extended in Hapke (1984) to take macroscopic roughness into account. The equations developed in these two papers are seen to remain valid, provided (52) and (53) are used wherever $B(g)$ appears, instead of the less rigorous expression for $B(g)$ originally given in those papers. The scale of macroscopic roughness in Hapke (1984) must be interpreted as being larger than L, the scale height of the particle density distribution, and smaller than the resolution footprint of the detector on the surface.

To illustrate and apply the ideas of this paper, the theoretical expressions of Hapke (1981, 1984) with the new form of $B(g)$ were fitted to photometric measurements on several Solar System bodies. The observations are those of Whitaker (1969) for the Moon, Bowell and Lumme (1979) for the asteroid 69 Hesperia, and Brown and Cruikshank (1983) for Uranus' satellite Oberon; Europa is also discussed.

The results of this analysis are shown in Fig. 6, along with values of h for which the theory gave a good fit. Assuming a regolith with a power-law particle size distribution characterized by $\beta = 4$ and $r_l/r_s = 1000$, we obtain the following values for the filling factor F. For the Moon, $h = 0.05$, giving $F = 0.41$. Values for Apollo lunar soil sam-

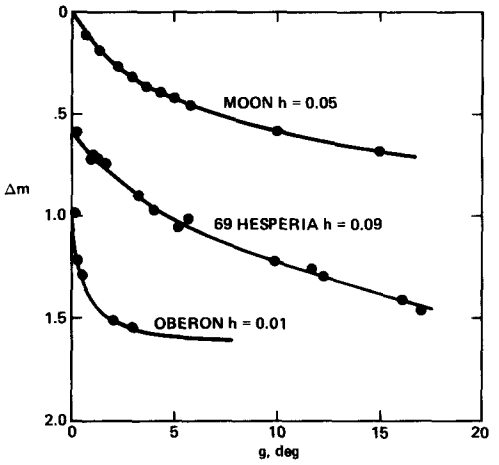

FIG. 6. The opposition effect in magnitudes versus phase angle g for three bodies of the Solar System. The dots are data and the lines are the theoretical function of this paper with the angular width parameter h as indicated. The data are arbitrarily normalized.

ples measured in terrestrial laboratories range from 0.27 to 0.65 (Carrier *et al.*, 1973). For 69 Hesperia, $h = 0.09$, giving $F = 0.61$, which is within the range of lunar soils. For Oberon, $h = 0.01$, giving $F = 0.10$. This value is in the range of filling factors of freshly deposited terrestrial snow, which has measured values of F ranging from 0.01 to 0.25, or natural graupel with F between 0.1 and 0.3 (Hobbs, 1974). Other values of F are possible, depending on the size distribution assumed. However, no bizarre particles or unknown microstructures need be postulated on the surface of the satellites of Uranus in order to account for the narrowness of their opposition peaks.

Millis and Thompson (1975) noted that Europa has a small or nonexistent opposition effect. Buratti (1985) has interpreted Voyager and Earth-based data as implying that Europa has a small opposition effect with an angular half-width of the order of 20°. Such a broad peak is difficult to distinguish from the general phase function of the body and could arise from other causes, such as macroscopic roughness (Hapke, 1984); hence, there is some doubt whether it is a true opposition effect or not. A true peak this broad could be understood if the regolith is not the result of comminution, but of some other process that gives a well-sorted grain size distribution. This would imply that $F \sim \frac{1}{3}$. An alternative possibility is that the surface is covered with a porous, dendritic frost of such low bulk density that the true peak is extremely narrow and has not yet been detected. More observations at very small phase angles are desirable, especially in the UV, where the albedo is low and multiple scattering effects are negligible.

VII. SUMMARY AND CONCLUSIONS

The extinction coefficient of a particulate medium has been shown to be given by

$$E = -n\langle\sigma\rangle \ln(1 - F)/F, \qquad (11)$$

where n is the particle density, $\langle\sigma\rangle$ is the average particle extinction cross section weighted by number, F is the filling factor $F = n\langle V\rangle$, and $\langle V\rangle$ is the average particle volume weighted by number. This expression for E is more accurate at large F than the commonly used expression $E = n\langle\sigma\rangle$, which is valid only when $F \ll 1$. The common expression for E can be retained if n is replaced by an effective particle density n_e, where

$$n_e = -n \ln(1 - F)/F. \qquad (12)$$

Similarly, the scattering coefficient is $n_e\langle\sigma_s\rangle$ and the absorption coefficient is $n_e\langle\sigma_a\rangle$, where $\langle\sigma_s\rangle$ and $\langle\sigma_a\rangle$ are, respectively, the average particle scattering and absorption cross sections weighted by number.

The opposition effect is caused by the hiding of extinction shadows and does not require that the particles be opaque. It can be described to a good approximation by multiplying the singly scattered radiance by a function of the phase angle g of the form

$$1 + B(g) = 1 + B_0/[1 + \tan(g/2)/h]. \qquad (52)$$

In this expression

$$B_0 = S(0)/wp(0), \qquad (53)$$

where w is the average single scattering albedo, $p(g)$ is the average particle angular scattering function, and $S(0)$ is the fraction

of $wp(g)$ that is scattered at $g = 0$ from the surface or near subsurface of the particle.

The angular half-width of the opposition peak is $\Delta g = 2h$, where

$$h = n_e(1)\langle\sigma\rangle\langle r\rangle/2, \quad (56)$$

$\langle r\rangle = \sqrt{\langle\sigma\rangle/\pi}$, and $n_e(1)$ is the value of n_e at the level in the medium where the slant path optical depth is approximately unity. In interpreting photometric data, it must be emphasized that $n_e(1)$ may be considerably different from the value of particle density n that controls other quantities, such as the bearing strength of the soil. Physically, the angular half-width is equal to the ratio of mean particle radius $\langle r\rangle$ to the extinction length $1/E$. The angular width parameter h is strongly dependent on the particle size distribution (Table I).

These theoretical equations fit observational data well. The value of F predicted for lunar regolith from the width of the Moon's opposition effect is in good agreement with measured values on Apollo soils. Physically reasonable values of F are predicted for 69 Hesperia and Oberon. Careful photometric observations of Europa at small phase angles could give important information about the microstructure of the regolith.

ACKNOWLEDGMENTS

Portions of this work were carried out while the author was a National Research Council, National Academy of Sciences Fellow at the Space Science Division, NASA Ames Research Center. The research was also supported by a grant from the National Aeronautics and Space Administration Planetary Geology and Geophysics Program.

REFERENCES

BHATTACHARYA, S., J. GOSWAMI, D. LAL, P. PATEL, AND M. RAO (1975). Lunar regolith and gas rich meteorites: Characterization based on particle tracks and grain size distribution. *Proc. Lunar Sci. Conf. 6th*, 3509–3526.

BOBROV, M. (1962). Generalization of the theory of the shadow effect on Saturn's rings to the case of particles of unequal size. *Sov. Astron. Astrophys. J.* **5**, 508–516.

BOWELL, E., AND K. LUMME (1979). Polarimetry and magnitudes of asteroids. In *Asteroids* (T. Gehrels, Ed.), pp. 132–169. Univ. of Arizona Press, Tucson.

BROWN, H., AND D. CRUIKSHANK (1983). The Uranian satellites: Surface compositions and opposition brightness surges. *Icarus* **55**, 83–92.

BURATTI, B. (1985). Application of a radiative transfer model to bright icy satellites. *Icarus* **61**, 208–217.

CARRIER, W., J. MITCHELL, AND A. MAHMOOD (1973). The relative density of lunar soil. *Proc. Lunar Sci. Conf. 4th*, 2403–2411.

DWIGHT, H. (1947). *Tables of Integrals and Other Mathematical Data*. MacMillan, New York.

EGAN, W., AND T. HILGEMAN (1976). Retroreflectance measurements of photometric standards and coatings. *Appl. Opt.* **15**, 1845–1849.

ESPOSITO, L. (1979). Extensions to the classical calculation of the effect of mutual shadowing in diffuse reflection. *Icarus* **39**, 69–80.

GEHRELS, T., T. COFFEEN, AND D. OWINGS (1964). Wavelength dependence of polarization. III. The lunar surface. *Astron. J.* **69**, 826–852.

GOGUEN, J. (1981). *A Theoretical and Experimental Investigation of the Photometric Functions of Particulate Surfaces*. Ph.D. thesis, Cornell University, Ithaca.

HAPKE, B. (1963). A theoretical photometric function for the lunar surface. *J. Geophys. Res.* **68**, 4571–4586.

HAPKE, B. (1981). Bidirectional reflectance spectroscopy. 1. Theory. *J. Geophys. Res.* **86**, 3039–3054.

HAPKE, B. (1984). Bidirectional reflectance spectroscopy. 3. Correction for macroscopic roughness. *Icarus* **59**, 41–59.

HAPKE, B., AND H. VAN HORN (1963). Photometric studies of complex surfaces with applications to the Moon. *J. Geophys. Res.* **68**, 4545–4570.

HAPKE, B., AND E. WELLS (1981). Bidirectional reflectance spectroscopy. 2. Experiments and observations. *J. Geophys. Res.* **86**, 3055–3060.

HOBBS, P. (1974). *Ice Physics*. Clarendon, Oxford.

IRVINE, W. (1966). The shadowing effect in diffuse reflectance. *J. Geophys. Res.* **71**, 2931–2937.

LUMME, K., AND E. BOWELL (1981). Radiative transfer in the surfaces of atmosphereless bodies. I. Theory. *Astron. J.* **86**, 1694–1704.

MILLIS, R., AND D. THOMPSON (1975). UBV photometry of the Galilean satellites. *Icarus* **26**, 408–419.

MONTGOMERY, W., AND R. KOHL (1980). Opposition-effect experimentation. *Opt. Lett.* **5**, 546–548.

OETKING, P. (1966). Photometric studies of diffusely reflecting surfaces with applications to the brightness of the Moon. *J. Geophys. Res.* **71**, 2505–2513.

SEELIGER, H. (1887). Zur Theorie der Beleuchtung der grossen Planeten Insbesondere des Saturn. *Abhandl. Bayer. Akad. Wiss. Math.-Naturw. Kl. II* **16**, 405–516.

SEELIGER, H. (1895). Theorie der Beleuchtung staubformiger kosmischen Masses Insbesondere des Sa-

turinges. *Abandl. Bayer. Akad. Wiss. Math.-Naturw. Kl. II* **18,** 1–72.

THORPE, T. (1978). Viking Orbiter observations of the Mars opposition effect. *Icarus* **36,** 204–215.

TROWBRIDGE, T. (1978). Retroreflection from rough surfaces. *J. Opt. Soc. Amer.* **68,** 1225–1242.

WHITAKER, E. (1969). An investigation of the lunar heiligenschein. In *Analysis of Apollo 8 Photography and Visual Observations,* pp. 38–39. NASA SP-201.

WHITAKER, E. (1979). Implications for asteroidal regolith properties from comparisons with the lunar phase relation and theoretical considerations. *Icarus* **40,** 406–417.

WILDEY, R. (1978). The Moon in heiligenschein. *Science* **200,** 1265–1267.